

Functionally pathogenic *EARS2* variants in vitro may not manifest a phenotype in vivo

OPEN

Nathan McNeill, PhD*
Alessia Nasca, MS
Aurelio Reyes, PhD
Benjamin Lemoine, MS
Brandi Cantarel, PhD
Adeline Vanderver, MD
Raphael Schiffmann,
MD*
Daniele Ghezzi, MD*

Correspondence to
Dr. McNeill:
Nathan_mcneill@alumni.baylor.edu

ABSTRACT

Objective: To investigate the genetic etiology of a patient diagnosed with leukoencephalopathy, brain calcifications, and cysts (LCC).

Methods: Whole-exome sequencing was performed on a patient with LCC and his unaffected family members. The variants were subject to in silico and in vitro functional testing to determine pathogenicity.

Results: Whole-exome sequencing uncovered compound heterozygous mutations in *EARS2*, c.328G>A (p.G110S), and c.1045G>A (p.E349K). This gene has previously been implicated in the autosomal recessive leukoencephalopathy with thalamus and brainstem involvement and high lactate (LTBL). The p.G110S mutation has been found in multiple patients with LTBL. In silico analysis supported pathogenicity in the second variant. In vitro functional testing showed a significant mitochondrial dysfunction demonstrated by an ~11% decrease in the oxygen consumption rate and ~43% decrease in the maximum respiratory rate in the patient's skin fibroblasts compared with the control. *EARS2* protein levels were reduced to 30% of normal controls in the patient's fibroblasts. These deficiencies were corrected by the expression of the wild-type *EARS2* protein. However, a further unrelated genetic investigation of our patient revealed the presence of biallelic variants in a small nucleolar RNA (*SNORD118*) responsible for LCC.

Conclusions: Here, we report seemingly pathogenic *EARS2* mutations in a single patient with LCC with no biochemical or neuroimaging presentations of LTBL. This patient illustrates that variants with demonstrated impact on protein function should not necessarily be considered clinically relevant.

ClinicalTrials.gov identifier: NCT00001671. **Neurol Genet** 2017;3:e162; doi: 10.1212/NXG.000000000000162

GLOSSARY

LCC = leukoencephalopathy, brain calcifications, and cysts; **LTBL** = leukoencephalopathy with thalamus and brainstem involvement and high lactate; **MAF** = minor allele frequency; **MRR** = maximum respiratory rate; **OCR** = oxygen consumption rate.

Leukodystrophies and genetic leukoencephalopathies are a heterogeneous group of rare inheritable neurologic diseases predominantly affecting the white matter of the brain.¹ Specific genetic diagnosis of these disorders was previously found in only about half of the known cases,² but next-generation sequencing has helped to increase the rate of genetic classification up to 80%.³

Next-generation sequencing has been successfully used in the identification of rare mutations in a number of genes causing many different white matter diseases and mitochondrial disorders.⁴ Particularly, mutations in the nuclear-encoded aminoacyl tRNA synthetase genes (ARSs) have been implicated in numerous mitochondrial disorders that cause white matter abnormalities.⁵ However, the explosive increase in rare genetic variants reported in the population in recent

See editorial

Supplemental data
at Neurology.org/ng

*These authors contributed equally to this work.

From the Baylor Research Institute (N.M., B.L., R.S.), Baylor Scott and White Health, Dallas, TX; Unit of Molecular Neurogenetics (A.N., D.G.), Foundation IRCCS Institute of Neurology "Besta," Milan, Italy; Mitochondrial Biology Unit (A.R.), Medical Research Council, Cambridge, United Kingdom; Department of Bioinformatics (B.C.), University of Texas Southwestern Medical Center, Dallas; and Department of Neurology (A.V.), George Washington University School of Medicine, Children's National Health, DC.

Funding information and disclosures are provided at the end of the article. Go to Neurology.org/ng for full disclosure forms. The Article Processing Charge was funded by the authors.

This is an open access article distributed under the terms of the Creative Commons Attribution-NonCommercial-NoDerivatives License 4.0 (CC BY-NC-ND), which permits downloading and sharing the work provided it is properly cited. The work cannot be changed in any way or used commercially without permission from the journal.

years has at times misrepresented the link between mutation and disease by incorrectly labeling many genetic variants as pathogenic.⁶ This is in part due to the lack of experimental validation of the pathogenicity of variants through functional in vitro or in vivo experimentation. Thus, clinical reporting of such variants is reliant on accurate information about the nature of the variant highlighting the importance of aggregated population databases for correct assessment of variant frequencies and the need for rigorous functional assays. As such, mitochondrial dysfunction can be ascertained through functional mitochondrial respiration assays, which are thought to be helpful in predicting DNA variant pathogenicity. However, functionally validated variants may not always be clinically relevant to the pathogenesis of the disease in question.

METHODS Standard protocol approvals, registrations, and patient consents. This study was approved to use human subjects by the appropriate institutional review board. Biological samples from the patient and first-degree relatives were collected subsequent to written informed consent; ClinicalTrials.gov identifier: NCT00001671. It included a family consisting of 2 parents and their affected son and his 3 unaffected siblings.

Whole-exome sequencing. Each family member was subjected to whole-exome sequencing and genetic analysis. Briefly, libraries were constructed from genomic DNA of each family member using the Illumina TruSeq DNA Sample Prep methodology (Illumina, San Diego, CA), and exonic targets were captured using Illumina's TruSeq Exome Enrichment technology according to the manufacturer's protocols. 2 × 50 bp paired-end sequencing was performed on the Illumina HiSeq 2000.

Bioinformatic analysis. Sequence reads were aligned to the human reference genome hg19 using the Burrows-Wheeler Aligner v.0.5.9.⁷ PCR duplicates were marked and removed using Picard v.1.70 (broadinstitute.github.io/picard/), and local realignment, quality score recalibration, and SNP and INDEL variant calling were performed using the Genome Analysis Toolkit v.1.3.⁸ The variant calls were subsequently annotated by Annovar.⁹ The gene annotations were made against the RefSeq database, and known variants and allele frequencies were annotated with dbSNP 137, all ethnicities from the 1000 Genomes Project (April 2012, August 2015 release), the National Heart, Lung, and Blood Institute (NHLBI) GO Exome Sequencing Project (ESP, esp6500 release), and the Exome Aggregation Consortium (ExAC). Nonsynonymous variants were further annotated with pathogenicity prediction scores from SIFT,¹⁰ PolyPhen-2,¹¹ LRT, and MutationTaster.¹² Conservation scores from PhyloP, GERP, and PhastCons were provided by MutationTaster and Annovar. Multiple sequence alignments were performed with Clustal Omega in Uniprot (uniprot.org). Variant prioritization and candidate gene identification used an in-house workflow that stratified the variant annotation data and white matter disease association analysis with a recessive or dominant model of inheritance.

Sanger sequencing. The *EARS2* variants were validated using Sanger sequencing. Genomic DNA was amplified using primers that targeted the variant location and subsequently sequenced using Applied Biosystems' BigDye Terminator v1.1 Sequencing Kit chemistry on a 3130xl sequencer (Applied Biosystems-Thermo Fisher Scientific, Waltham, MA). In addition, the *EARS2* genes in 2 unrelated patients diagnosed with leukoencephalopathy, brain calcifications, and cysts (LCC) were Sanger sequenced using primers that spanned all 9 exons and exon-intron boundaries. PCR amplification was performed using HotStarTaq Master Mix (Qiagen, Hilden, Germany) according to the manufacturer's protocols. *EARS2* primers are listed in table e-1 at Neurology.org/ng.

Skin fibroblast cell culture and complementation studies.

Primary skin fibroblasts from the affected patient and controls were cultured in 1 × Dulbecco Modified Eagle Medium (Corning, Corning, NY) with 4.5 g/L glucose supplemented with L-glutamine and sodium pyruvate, 10% fetal bovine serum, and 1% antimyotic in a 25-cm² flask. The medium was changed every 2 days until 90%–100% confluent, at which time the cells were trypsinized with 0.25% or 0.05% trypsin and washed with 1 × phosphate-buffered saline (Gibco-Thermo Fisher Scientific) without Ca²⁺/Mg²⁺ then subpassaged to a 75 cm² flask. Cultures were maintained in a humidified atmosphere at 37°C with 5% CO₂.

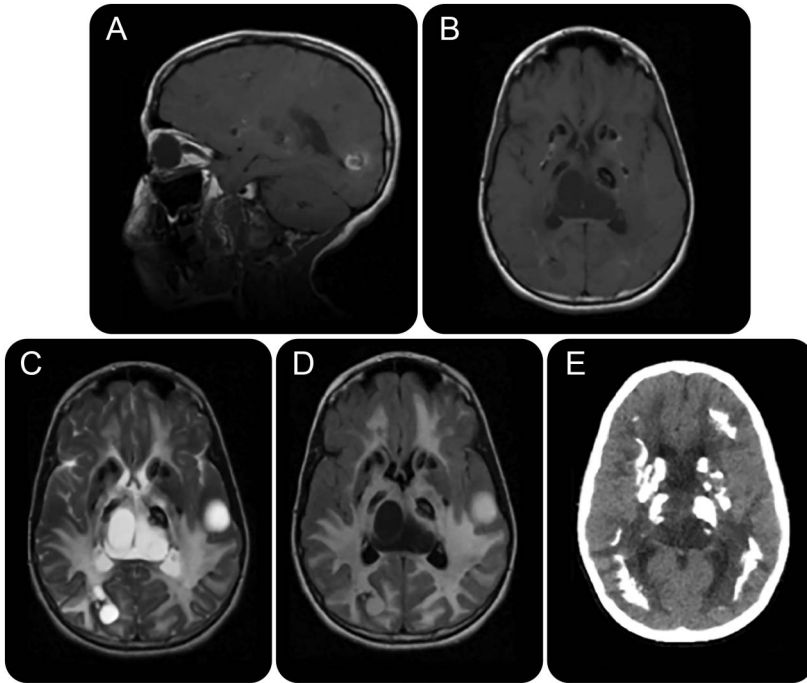
Fibroblasts were immortalized with pRNS-1 by transfection using Lipofectamine2000 (Invitrogen-Thermo Fisher Scientific) and selected by 100 μg/mL Geneticin G-418 (Gibco-Thermo Fisher Scientific).¹³ For complementation, wild-type (wt) cDNAs of *EARS2* from a commercial clone (OCAAo5051A02110D) (Source BioScience, Nottingham, United Kingdom) were cloned into the pLenti6.2/V5 TOPOVector (Life Technologies-Thermo Fisher Scientific), and virions were obtained as previously described.¹⁴ Mutant and control immortalized fibroblasts were transfected with viral supernatant and selected upon exposure to 2 μg/mL Blasticidin (Life Technologies-Thermo Fisher Scientific).

Western blot protein expression. Fibroblasts and immortalized cells from patient and controls were trypsinized, pelleted, and solubilized in RIPA buffer with protease inhibitors; 50 μg of protein was loaded for each sample in 12% denaturing sodium dodecyl sulfate polyacrylamide gel electrophoresis. A rabbit polyclonal antibody against EARS2 (SAB2100641) (Sigma-Aldrich, St. Louis, MO) and a mouse monoclonal antibody against GAPDH (#MAB374) (Millipore, Billerica, MA) were used.

Mitochondrial respiration assays. Oxygen consumption rate (OCR) and maximum respiratory rate (MRR) were measured using a SeaHorse FX-96 apparatus (Agilent Technologies, Santa Clara, CA)¹⁵ in primary fibroblasts and immortalized fibroblasts in naive conditions and after transduction with wild-type *EARS2* cDNA.

RESULTS Clinical profile. A 6-year-old male patient born to healthy nonconsanguineous parents presented with a progressive encephalopathy consisting of intractable seizures, dystonia, chorea, and spasticity with severely impaired cognitive function. MRI (figure 1, A–D) and CT (figure 1E) showed diffuse white matter signal abnormalities and numerous calcifications throughout the brain in gray matter nuclei and juxtacortical U-fibers as well as the

Figure 1 Patient with leukoencephalopathy brain imaging



MRIs (A–D) and CT (E) indicate white matter signal abnormalities, cysts, and calcifications throughout the cerebral hemispheres. Diffuse cerebral white matter lesions are present, which is demonstrated by hypointense signals in the sagittal (A) and axial T1-weighted (B) images and the CT (E) and by the hyperintense signals in the axial T2-weighted (C) and axial fluid-attenuated inversion recovery (FLAIR) images. The CT (E) shows extensive calcifications in the subcortical white matter and along the periventricular white matter. Large cystic lesions can be seen along the quadrigeminal plane and parieto-occipital regions (B–D).

periventricular white matter, brainstem, the dentate nucleus of the cerebellum, and the subcortical white matter of both cerebral hemispheres. White matter abnormalities were observed through increased signals in the white matter in T2-weighted (figure 1C) and fluid-attenuated inversion recovery (FLAIR) (figure 1D) images and decreased signals on sagittal (figure 1A) and T1-weighted images (figure 1B). MR spectroscopy showed decrease in N-acetyl aspartate and no lactate peak. A number of large cysts were also present in the cerebellum and the supratentorial region (figure 1, A–D). Anatomically, lateral ventricles were enlarged with a missing septum pellucidum, atrophy of the corpus callosum, and basal ganglia volume loss. Routine laboratory testing revealed normal values and complete blood count. Extensive biochemical investigations were all normal except for a CNS folate deficiency from decreased concentrations of 5-MTHF of unknown cause. Muscle biopsy demonstrated a normal histopathology and mitochondria that were normal in number, distribution, and morphology with no mtDNA abnormalities. Cellular lactate-to-pyruvate ratio was normal in cultured skin fibroblasts. Skeletal muscle showed normal carnitine profiles and normal activity of the electron transport chain complexes I, II, III, and IV

with citrate synthase at the upper limits of normal, which may indicate an increase in mitochondrial content. Glucose, lactate, and total protein were normal in the CSF.

The patient died at 16 years of age. Autopsy showed that the entire CNS was devastated by a vasculopathy with secondary ischemic lesions and mineralization, leading to the progressive obliteration of the blood vessel lumina and gliosis resulting in the presence of Rosenthal fibers. Necrosis, dystrophic calcifications, white matter degeneration, and cyst formation were found. There were no abnormalities outside the CNS. The patient was diagnosed with the cerebral microangiopathy LCC.¹⁶ LCC is a rare disorder, as fewer than 50 cases have ever been reported in the literature.¹⁷

Exome sequencing and genetic analysis. Whole-exome sequencing generated an average of 3.2 Gb of sequence and 61–73 million reads per individual that mapped uniquely to the genome with a mean sequence coverage of 26×. LCC is an assumed autosomal recessive disorder due to the occurrence of sibling pairs, which include females, but variants following both an autosomal recessive and autosomal dominant inheritance pattern were interrogated. Following a candidate gene prioritization and filtering strategy that enriched for rare (minor allele frequency [MAF] of <1%) nonsynonymous exonic/splice variants that both segregated in a recessive or dominant manner and may or may not be associated with white matter disease pathogenesis, only 2 recessive variants in the *EARS2* gene segregated in a compound heterozygous manner, c.328G>A (p.Gly110Ser) and c.1045G>A (Glu349Lys). No other obvious exonic or splice variants were observed. The presence or absence of the 2 variants and their segregation within the family were validated with Sanger sequencing (figure e-1). The patient was compound heterozygous for the 2 variants, the mother was heterozygous for the c.328G>A variant, and the father was heterozygous for the c.1045G>A variant. Two of the siblings were heterozygous for either variant. Sanger sequencing of the exon and exon/intron boundaries of *EARS2* in 2 unrelated patients with LCC revealed only common polymorphisms and no rare mutations.

In silico analysis of *EARS2* variants. The *EARS2* variants were analyzed in silico to determine the MAF within the population, predicted pathogenicity, and evolutionary conservation. The c.1045G>A nucleotide resides in exon 5 of *EARS2* in the anticodon binding domain, resulting in a missense amino acid change from a large acidic negatively charged glutamic acid to a large positively charged basic lysine at residue 349 (Grantham Score: 56). It was present at low frequencies in 1000 Genomes (MAF 0.10%), ESP (MAF

0.18%), and ExAC (MAF 0.13%). It was also present in dbSNP (rs#187662524). The variant was predicted as benign by PolyPhen-2, damaging or disease causing by SIFT and MutationTaster, and neutral by LRT. This position is conserved according to GERP, PhyloP, and PhastCons.

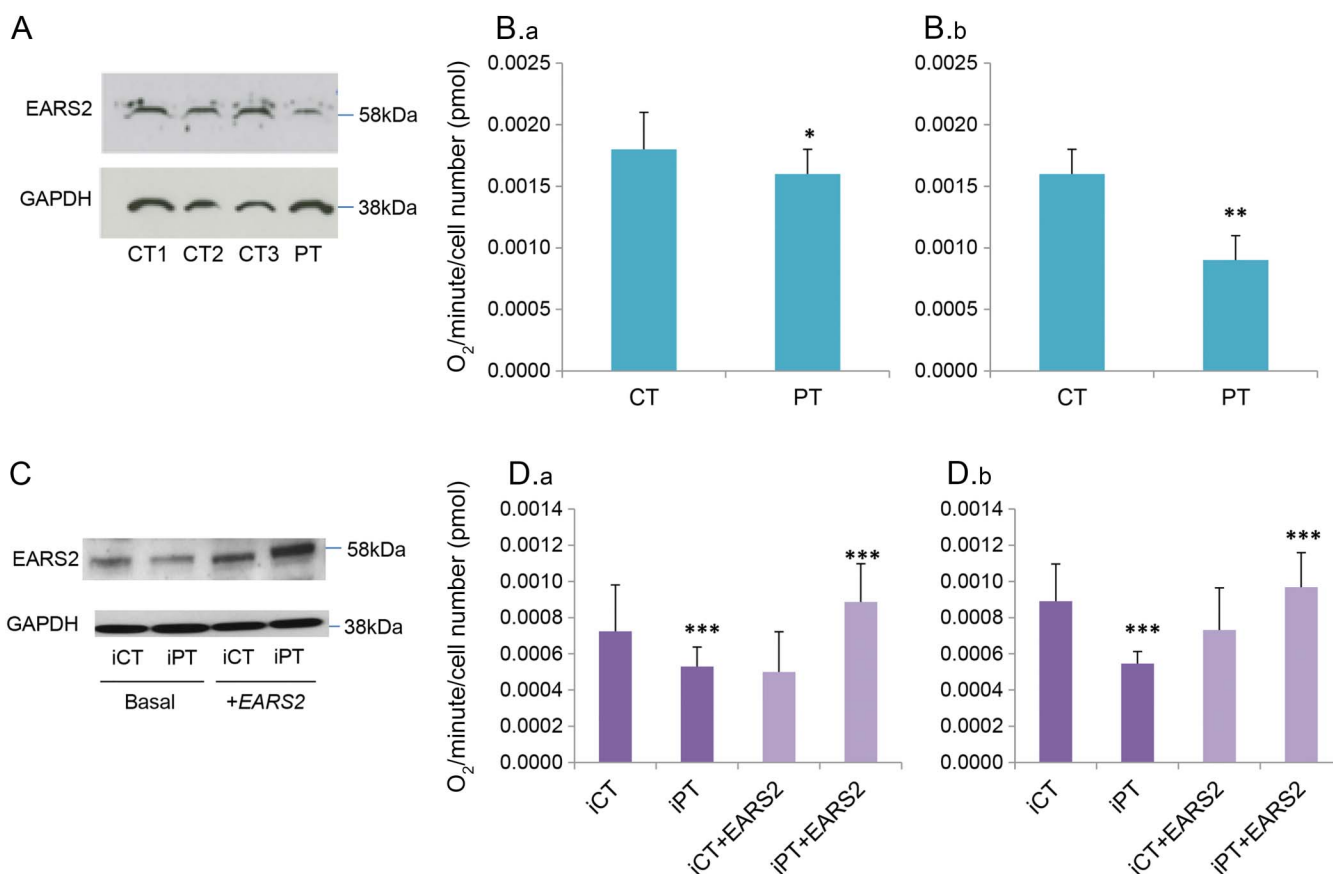
The c.328G>A nucleotide change resides in exon 3 in the catalytic domain of *EARS2*, resulting in a missense amino acid change from a small polar glycine to a small polar serine at residue 110 (Grantham Score: 56). It was not present in the 1000 Genomes, but it was present at low frequencies in the ESP (MAF 0.03%) and ExAC (MAF 0.04%) databases. It was also present in dbSNP (rs#201842633). Pathogenicity prediction programs considered this variant as damaging/disease causing by SIFT, PolyPhen2, MutationTaster, and LRT. GERP, PhyloP, and PhastCons also predicted high conservation at this position.

Multiple sequence alignment (figure e-2) showed that the G110 residue is invariant from humans

through *Caenorhabditis elegans*, and the E349 residue showed amino acid class conservation through *C. elegans*. The c.328G>A variant was also found in 3 other unrelated patients with leukoencephalopathy with thalamus and brainstem involvement and high lactate (LTBL),^{18,19} whereas the c.1045G>A variant has never been reported to be associated with human diseases. According to the ACMG and AMP recommended guidelines for interpreting sequence variants, both variants demonstrate evidence for pathogenicity.²⁰

Biochemical/protein studies on patient's fibroblasts. Skin fibroblasts from the proband were analyzed to evaluate the effect of the identified *EARS2* variants. The total amount of *EARS2* protein detected by Western blot analysis was reduced to 30% in the patient's fibroblasts compared with controls (figure 2A). Oxygen consumption, which depends on and reflects the cumulative proficiency of the whole set of

Figure 2 Functional characterization of *EARS2* variants on fibroblasts



(A) *EARS2* protein amount in the patient's (Pt) and control (CT1, CT2, and CT3) fibroblasts, obtained by Western blot using an anti-*EARS2* antibody. An anti-GAPDH antibody was used as a loading control. (B) Oxygen consumption analysis in the patient's (Pt) and control fibroblasts. Histograms show OCR (B.a and D.a) and MRR (B.b and D.b). OCR and MRR values (mean of 6-8 replicates) are expressed as picomoles of O_2 per minute and normalized by cell number. *p* value obtained with 2-tailed Student *t* test, **p* < 0.05; ***p* < 0.01. (C) *EARS2* protein amount in the patient's (iPt) and control (iCT) immortalized fibroblasts, in basal conditions and after transduction with wt *EARS2* (+*EARS2*); Western blot analysis was performed as described in A. (D) Oxygen consumption analysis, as reported in B, performed in patient's (iPt) and control (iCT) immortalized fibroblasts, in basal conditions and after transduction with wild-type *EARS2* (+*EARS2*). ****p* < 0.001. MRR = maximum respiration rate; OCR = oxygen consumption rate.

mitochondrial respiratory chain complexes, was measured. Significant reductions of both OCR and MRR, indicating reduced electron flow through the respiratory chain, were observed (figure 2B). These alterations were also confirmed in patient-derived immortalized fibroblasts (figure 2, C and D), which were then used for complementation through transduction of wild-type *EARS2*. Overexpression of *EARS2* protein in both control and mutant transduced cells (figure 2C) was associated with the recovery of defective respiratory parameters (OCR and MRR) to normal values (figure 2D).

DISCUSSION Using whole-exome sequencing and ad hoc strategic filtering with integration of gene information and disease association, 2 rare *EARS2* (MIM 612799) mutations were observed to be segregating in a compound heterozygous manner within a single family with an individual presenting with LCC (MIM 614561; Labrune Syndrome). *EARS2* is targeted to the mitochondria and functions as a crucial component of mitochondrial translation by catalyzing the ligation of glutamate to its cognate tRNA molecule; however, all its functions have not yet been elucidated. Previous genetic studies identified mutations in *EARS2* as the cause of combined oxidative phosphorylation deficiency 12 (COXPD12), also known as LTBL (MIM 614924).¹⁸ Biochemical and neuroimaging features of LTBL associated with *EARS2* mutations include characteristic lactate elevation in MR spectroscopy and body fluids, variable corpus callosum involvement, and symmetric white matter signal abnormalities in the cerebral white matter, thalami, brainstem, and cerebellar white matter with sparing of the periventricular rim (figure 3, A–D).^{18,19}

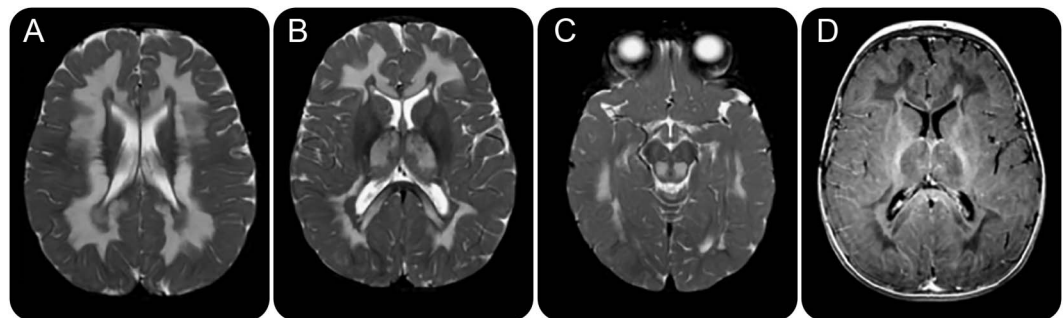
Conversely, LCC is strictly a neurologic disorder limited to the CNS and consisting of a cerebral microangiopathy resulting in presumed tissue hypoxia,

which leads to microcystic and macrocystic parenchymal degeneration with white matter changes secondary to brain edema rather than primary demyelination.^{16,17,21} MRI of the patient was consistent with LCC and not LTBL. The patient's pathology was also consistent with LCC including angiomatous-like rearrangements of microvessels with secondary degeneration of cellular constituents such as gliosis and aggregates of intermediate filaments called Rosenthal fibers,^{16,22} none of which are known to be found in LTBL. LCC and LTBL have strikingly different neuroimaging and pathologic features, suggesting that *EARS2* is not involved in the pathogenesis of LCC.

However, functional studies on the LCC patient's fibroblasts clearly demonstrated a mitochondrial dysfunction due to abnormal mitochondrial respiration with significantly decreased MRR and OCR and decreased *EARS2* protein levels suggestive of a pathogenic role of the *EARS2* variants; nonetheless, LCC does not present with mitochondrial abnormalities. Abnormal mitochondrial respiration and decreased protein levels as seen in this patient have both been confirmed in other patients with LTBL.^{18,19,23} Patients with LTBL have seen up to a ~70% decrease in the MRR,¹⁸ and our patient showed a less severe but still a significant decrease of ~43% in the MRR. Despite these abnormalities, increased lactate, which is a hallmark of LTBL and a consequence of pathogenic *EARS2* mutations,^{18,19} was not seen in MR spectroscopy or body fluids in the present patient with LCC.

Recently, mutations in the *SNORD118* gene located in the 3' UTR region of the *TMEM107* gene were identified in the pathogenesis of LCC.²⁴ *SNORD118* encodes the box C/D snoRNA U8 important for ribosome biosynthesis. In that publication, family member 1A from family F278, which was this study's patient with LCC, was found to have

Figure 3 LTBL brain imaging



Axial T2-weighted (A–C) and T1-weighted (D) MRIs demonstrate T2-hyperintensities and T1-hypointensities respectively, indicating lesions in the deep cerebral white matter and periventricular white matter with sparing of the periventricular rim. Signal hyperintensities are also present in the thalami (B) and dorsal part of the midbrain (C). Modified from reference 18. LTBL = leukoencephalopathy with thalamus and brainstem involvement and high lactate.

compound heterozygous mutations in *SNORD118*: a novel n.75A>G mutation and a very rare n.8G>C mutation. The presence of the *SNORD118* mutations as the pathogenic driver of LCC relegates the functionally pathogenic *EARS2* variants in this case to an unknown status; however, *EARS2* as a genetic disease modifier or the additional presence of protective alleles from defective *EARS2* cannot be ruled out.

The absence of a clear LTBL phenotype in a patient with apparent functionally validated pathogenic *EARS2* variants, and the presence of other pathogenic variants (i.e., *SNORD118* mutations) strongly associated with the patient's phenotype, throws doubt on our ability to infer the clinical pathogenic effect of a variant through in vitro experiments. According to the standards and guidelines for the interpretation of sequence variants set in place by the American College of Medical Genetics and Genomics (ACMG),²⁰ the *EARS2* variants are considered pathogenic on their own and should be labeled as such in clinical reports. The functional assays indicating mitochondrial dysfunction through respiration defects as presented in this study are typically sufficient to demonstrate clinical relevance of *EARS2* variants¹⁸ and other variants in mitochondrial-related genes.^{25,26} It is important that this indicates that one cannot simply always assume that putative functionally damaging variants ascertained from in vitro experimentation are clinically relevant. In vitro observations about the deleterious effects of a given variant on biochemical functionalities do not necessarily translate to in vivo pathogenicity or strict clinical causality; a second, possibly more relevant, genetic or epigenetic factor should always be taken into account, especially for cases with previously unreported genotype/phenotype correlations. This further complicates the pathogenic validation of rare genetic variants and their role in disease, underscoring the need for more robust and precise validation methods.

AUTHOR CONTRIBUTIONS

N.H.M. conceived and designed the study and experiments; performed sample preparation; performed bioinformatics and statistical analysis of sequence data; performed bioinformatics analysis of *EARS2* variants; performed mutation analysis and Sanger sequencing; performed fibroblast cell culture; drafted the manuscript; and edited the manuscript. A.N. performed cell culture, Western blot, and Seahorse assays and analyzed data. AR performed the immortalization. B.L. performed sample preparation and whole-exome sequencing. B.C. performed bioinformatics analysis of sequence data. A.V. acquired and assessed the patient; provided an additional patient for Sanger sequencing; and edited the manuscript. R.S. conceived and designed the study and experiments; acquired and assessed the patient; and edited the manuscript. D.G. conceived and designed the study and experiments; analyzed the Seahorse data and Western blot data; and edited the manuscript.

ACKNOWLEDGMENT

The authors thank the study subjects for their participation and consent. They also thank Dr. Marjo van der Knaap for providing an additional patient for Sanger sequencing.

STUDY FUNDING

Funding provided by the Baylor Scott & White Healthcare Foundation.

DISCLOSURE

N. McNeill, A. Nasca, A. Reyes, B. Lemoine, and B. Cantarel report no disclosures relevant to the manuscript. A. Vanderver has served on the scientific advisory board of Shire Pharmaceuticals; has received travel funding/speaker honoraria from Hunter's Hope (family foundation for Metachromatic Leukodystrophy), United Leukodystrophy Foundation, Metachromatic Leukodystrophy Foundation, and European Leukodystrophy Foundation; holds a patent (pending) for Sialic acid measurement in CSF in the diagnosis of Vanishing White Matter disease; has been an unpaid consultant for Stem Cells Inc.; and has received research support from Pennsylvania Department of Health, Frontiers in Leukodystrophy Initiative (FrontLINE), NIH, H-ABC Research Fund, Calendar Research Contribution Fund, H-ABC Research Fund, and Aicardi-Goutieres Syndrome Research Fund. R. Schiffman has served on the scientific advisory boards of and has received travel funding/speaker honoraria from Protalix Biotherapeutics and Amicus Therapeutics; holds the following patents: Triheptanoin diet for Adult Polyglucosan Body Disease (APBD), Use of tetrahydrobiopterin as a marker and a therapeutic agent for Fabry disease (3), Urinary triaolsylceramide (GB3) as a marker of cardiac disease, and Gene encoding a new TRP channel is mutated in mucopolipidosis; has been a consultant for Gerson Lehrman Group Councils and Guidepoint Global; has served on the speakers' bureau of Genzyme Corporation; and has received research support from Protalix Biotherapeutics, Amicus Therapeutics, and Baylor Research Foundation. D. Ghezzi has served on the editorial board of *Orphanet Journal of Rare Diseases*; and has received research support from the Italian Ministry of Health, European Communities, Foundation Telethon, CARIPLO Foundation Italy, and Pierfranco and Luisa Mariani Foundation of Italy. Go to Neurology.org/ng for full disclosure forms.

Received February 13, 2017. Accepted in final form April 18, 2017.

REFERENCES

1. Vanderver A, Prust M, Tonduti D, et al. Case definition and classification of leukodystrophies and leukoencephalopathies. *Mol Genet Metab* 2015;114:494–500.
2. Parikh S, Bernard G, Leventer RJ, et al. A clinical approach to the diagnosis of patients with leukodystrophies and genetic leukoencephalopathies. *Mol Genet Metab* 2015;114:501–515.
3. Kevelam SH, Steenweg ME, Srivastava S, et al. Update on leukodystrophies: a historical perspective and adapted definition. *Neuropediatrics* 2016;47:349–354.
4. Vanderver A, Simons C, Helman G, et al. Whole exome sequencing in patients with white matter abnormalities. *Ann Neurol* 2016;79:1031–1037.
5. Yao P, Fox PL. Aminoacyl-tRNA synthetases in medicine and disease. *EMBO Mol Med* 2013;5:332–343.
6. Lek M, Karczewski KJ, Minikel EV, et al. Analysis of protein-coding genetic variation in 60,706 humans. *Nature* 2016;536:285–291.
7. Li H, Durbin R. Fast and accurate short read alignment with Burrows-Wheeler transform. *Bioinformatics* 2009;25:1754–1760.
8. McKenna A, Hanna M, Banks E, et al. The Genome Analysis Toolkit: a MapReduce framework for analyzing next-generation DNA sequencing data. *Genome Res* 2010;20:1297–1303.
9. Wang K, Li M, Hakonarson H. ANNOVAR: functional annotation of genetic variants from high-throughput sequencing data. *Nucleic Acids Res* 2010;38:e164.
10. Kumar P, Henikoff S, Ng PC. Predicting the effects of coding non-synonymous variants on protein function using the SIFT algorithm. *Nat Protoc* 2009;4:1073–1081.

11. Adzhubei IA, Schmidt S, Peshkin L, et al. A method and server for predicting damaging missense mutations. *Nat Methods* 2010;7:248–249.
12. Schwarz JM, Cooper DN, Schuelke M, Seelow D. MutationTaster2: mutation prediction for the deep-sequencing age. *Nat Methods* 2014;11:361–362.
13. Litzkas P, Jha KK, Ozer HL. Efficient transfer of cloned DNA into human diploid cells: protoplast fusion in suspension. *Mol Cell Biol* 1984;4:2549–2552.
14. Zhang JC, Sun L, Nie QH, et al. Down-regulation of CXCR4 expression by SDF-KDEL in CD34(+) hematopoietic stem cells: an anti-human immunodeficiency virus strategy. *J Virol Methods* 2009;161:30–37.
15. Invernizzi F, D'Amato I, Jensen PB, Ravaglia S, Zeviani M, Tiranti V. Microscale oxygraphy reveals OXPHOS impairment in MRC mutant cells. *Mitochondrion* 2012;12:328–335.
16. Labrune P, Lacroix C, Goutieres F, et al. Extensive brain calcifications, leukodystrophy, and formation of parenchymal cysts: a new progressive disorder due to diffuse cerebral microangiopathy. *Neurology* 1996;46:1297–1301.
17. Stephani C, Pfeifenbring S, Mohr A, Stadelmann C. Late-onset leukoencephalopathy with cerebral calcifications and cysts: case report and review of the literature. *BMC Neurol* 2016;16:19.
18. Steenweg ME, Ghezzi D, Haack T, et al. Leukoencephalopathy with thalamus and brainstem involvement and high lactate “LTBL” caused by EARS2 mutations. *Brain* 2012;135:1387–1394.
19. Danhauser K, Haack TB, Alhaddad B, et al. EARS2 mutations cause fatal neonatal lactic acidosis, recurrent hypoglycemia and agenesis of corpus callosum. *Metab Brain Dis* 2016;31:717–721.
20. Richards S, Aziz N, Bale S, et al. Standards and guidelines for the interpretation of sequence variants: a joint consensus recommendation of the American College of Medical Genetics and Genomics and the Association for Molecular Pathology. *Genet Med* 2015;17:405–424.
21. Livingston JH, Mayer J, Jenkinson E, et al. Leukoencephalopathy with calcifications and cysts: a purely neurological disorder distinct from coats plus. *Neuropediatrics* 2014;45:175–182.
22. Corboy JR, Gault J, Kleinschmidt-DeMasters BK. An adult case of leukoencephalopathy with intracranial calcifications and cysts. *Neurology* 2006;67:1890–1892.
23. Oliveira R, Sommerville EW, Thompson K, et al. Lethal neonatal LTBL associated with biallelic EARS2 variants: case report and review of the reported neuroradiological features. *JIMD Rep* 2017;33:61–68.
24. Jenkinson EM, Rodero MP, Kasher PR, et al. Mutations in SNORD118 cause the cerebral microangiopathy leukoencephalopathy with calcifications and cysts. *Nat Genet* 2016;48:1185–1192.
25. Ghezzi D, Baruffini E, Haack TB, et al. Mutations of the mitochondrial-tRNA modifier MTO1 cause hypertrophic cardiomyopathy and lactic acidosis. *Am J Hum Genet* 2012;90:1079–1087.
26. Wong LJ. Mitochondrial syndromes with leukoencephalopathies. *Semin Neurol* 2012;32:55–61.